

## Growth of exchange-biased MnPd/Fe bilayers

P. Blomqvist and Kannan M. Krishnan<sup>a)</sup>

*Materials Science and Engineering, University of Washington, Seattle, Washington 98195*

David E. McCready

*Environmental Molecular Sciences Laboratory, Pacific Northwest National Laboratory, Richland, Washington 99352*

(Received 17 December 2003; accepted 1 March 2004)

The growth of exchange-biased MnPd/Fe bilayers has been investigated using x-ray diffraction. The bilayers were deposited on MgO<sub>(001)</sub> substrates in an ultrahigh-vacuum ion-beam sputter system. It was found that the orientation of the MnPd unit cell and the crystalline quality could be controlled as a function of the deposition temperature. Twinned *a*-axis oriented MnPd films are obtained below 100 °C while single-crystalline *c*-axis films are obtained above 450 °C. Intermediate temperatures yield a mixture of both orientations with a poor crystalline quality. Moreover, the interface quality depends strongly on the deposition temperature and also the order in which MnPd and Fe are deposited. The results clearly show that interdiffusion is initiated at the Fe/MnPd interface at a lower temperature as compared to the MnPd/Fe interface. The close relationship between the structural and magnetic properties is also discussed. © 2004 American Institute of Physics.  
[DOI: 10.1063/1.1713023]

### INTRODUCTION

The exchange bias effect was discovered in partly oxidized Co particles by Meiklejohn and Bean and has since been found in numerous ferromagnetic/antiferromagnetic systems, both in particles as well as in layered thin film structures.<sup>1-4</sup> The exchange coupling between the ferromagnet (FM) and the antiferromagnet (AFM) gives rise to a unidirectional anisotropy which manifests itself as a shift of the hysteresis loop. The application of the exchange bias effect in spin-valve magnetoresistance and magnetic random access memory devices has created a renewed research interest in this phenomenon during the past decade. It has been found experimentally that the magnitude of the bias and the coercivity is directly linked not only to the properties of the constituents but also to the properties of the FM/AFM interface. Important parameters include the overall crystallinity, spin configuration at the FM/AFM interface (spin-compensated interface versus uncompensated and in-plane versus out-of-plane AFM spins), magnetocrystalline anisotropy, FM/AFM interface disorder, and the thickness of the ferromagnetic and the antiferromagnetic layers.<sup>3,4</sup> Hence, it is essential to systematically correlate the structural details with the magnetic properties. This is best done with samples with well-defined crystal and interface structure. In this paper, we present a detailed study of epitaxially grown MnPd/Fe bilayers which exhibit a strong exchange bias effect. The temperature dependence of the crystal and interface structure has been investigated using x-ray diffraction (XRD). The close relationship between the structural and magnetic properties is also discussed.

<sup>a)</sup>Electronic mail: kannanmk@u.washington.edu

### EXPERIMENTAL DETAILS

All the samples were prepared on single-crystalline MgO<sub>(001)</sub> substrates in an ultrahigh-vacuum ion-beam sputter deposition system with a base pressure of 10<sup>-9</sup> Torr. The substrates were precleaned in acetone and ethanol and out-gassed at 500 °C for 10 min prior to deposition. The deposition rates for MnPd (composite alloy target) and Fe were ~0.2 and ~0.5 Å/s, respectively. The composition of the MnPd alloy in the samples was determined by energy dispersive x-ray analysis to be Mn(52 at.%)Pd(48 at.%). A magnetic field (300 Oe) was applied along the Fe<sub>[100]</sub> crystallographic direction (magnetic easy axis) during deposition. All the samples were capped with a Au layer to protect them against oxidation. Three x-ray-diffraction setups were used for the structural characterization of the samples. High-angle measurements were carried out on a Rigaku rotating-anode powder diffractometer, low-angle reflectivity measurements were performed using a Philips X'Pert MPD system with parallel beam optics, and a Philips X'Pert Pro MRD system with high-resolution optics was used for texture measurement. All three XRD systems were equipped with Cu K $\alpha$  x-ray sources. Magnetization measurements were performed at room temperature in a vibrating sample magnetometer.

### RESULTS AND DISCUSSIONS

MnPd is a chemically ordered L1<sub>0</sub> (CuAu I structure) antiferromagnetic alloy with a Néel temperature in the bulk of 540 °C. In this structure, Mn has a magnetic moment of 4.4  $\mu$ B (room-temperature value) with the easy axes along [100] and [-100] (or [010] and [0-10]) while the moment is vanishingly small for Pd. The MnPd unit cell is face-centered-tetragonal (fct) with lattice parameters of 3.58, 4.07, and 4.07 Å.<sup>5</sup> The distorted axis (the [001] direction) of the MnPd unit cell can be either in-plane or out-of-plane; if it

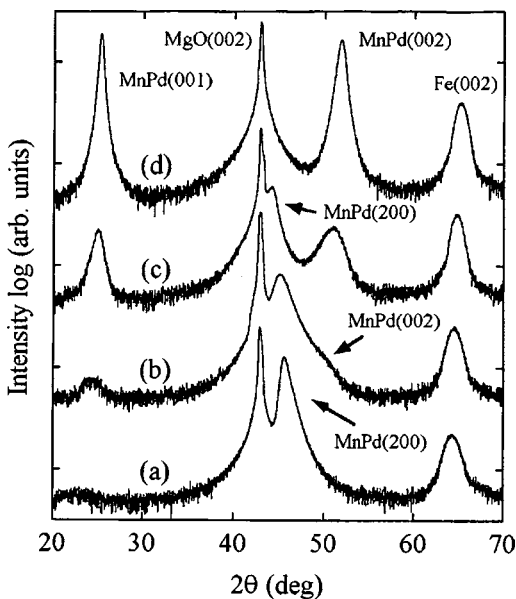


FIG. 1. High-angle XRD data from four Au(20 Å)/MnPd(330 Å)/Fe(80 Å)/MgO bilayers deposited at 100 °C (a), 200 °C (b), 350 °C (c), and 450 °C (d). The orientation of the MnPd film changes from a twinned *a*-axis to a single-crystalline *c*-axis orientation when the deposition temperature is increased from 100 °C to  $\geq 450$  °C.

is in-plane, the film is referred to as *a*-axis oriented, while it is said to be *c*-axis oriented if it is out-of-plane. It should be noted that the atomic planes perpendicular to the *c* axis are spin-compensated (zero net magnetic moment in the plane), whereas the planes perpendicular to the two *a* axes are spin-uncompensated. The fact that  $a_{\text{MgO}} \sim a_{\text{MnPd}}$  and  $a_{\text{MnPd}}/\sqrt{2} \sim a_{\text{Fe}}$  indicates that MnPd and Fe can be grown epitaxially on MgO(001).<sup>6,7</sup> This gives the following epitaxial relationships for the single-crystalline *c*-axis orientation: Fe[001]//MnPd[001]//MgO[001] and Fe[110]//MnPd[100]//MgO[100]. The *a*-axis orientation has a bicrystal orientation with the possibility of exhibiting a twinned crystal structure.

XRD scans ( $\theta$ - $2\theta$ ) from four MnPd/Fe bilayers with the nominal film structure Au(20 Å)/MnPd(330 Å)/Fe(80 Å)/MgO are shown in Fig. 1. They were deposited at 100 °C (a), 200 °C (b), 350 °C, (c) and 450 °C (d). The peaks at 42.9° and 65.0° are the MgO(002) and the Fe(002) reflections, respectively. The *c*-axis orientation can be identified by the MnPd(001) and MnPd(002) reflections, while the *a*-axis orientation is identified by the MnPd(200) (or MnPd(020)). As seen in the figure, the orientation of the MnPd unit cell depends strongly on the growth temperature. A mixture of both *a* and *c* axis is obtained over a large temperature interval ( $\sim 200$ – $350$  °C), whereas pure *a*-axis and *c*-axis orientation is obtained below 100 °C and above 450 °C, respectively. The presence of a MnPd(001) peak indicates that the *c*-axis oriented film is chemically ordered with alternating layers of Mn and Pd perpendicular to the film normal. It is not possible to say whether the *a*-axis orientation is chemically ordered or not since the scattering vector is parallel to the film normal in a symmetric  $\theta$ - $2\theta$  scan. This type of XRD scan is only sensitive to the crystalline structure in the out-of-plane direction. However, a transmission electron microscopy (TEM) study (plan view) with an in-plane scattering vector

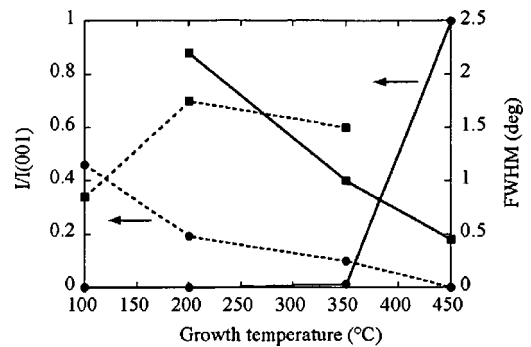


FIG. 2. Peak intensity and full width at half maximum (FWHM in the  $\theta$ - $2\theta$  direction) versus the deposition temperature for four different Au(20 Å)/MnPd(330 Å)/Fe(80 Å)/MgO bilayers are shown in the figure. Solid lines represent data for the MnPd(001) reflection and dashed lines are for the MnPd(200) reflection. The peak intensities have been normalized with the intensity of the MnPd(001) reflection.

has shown that a chemically ordered *a*-axis orientation can be obtained in MnPd/Fe/MgO(001) films if they are deposited at low enough temperatures and then annealed.<sup>6</sup> The samples in this study were not annealed after deposition, hence they are expected to be chemically disordered.

The intensity of an XRD reflection depends both on the sample volume and the crystalline quality. If the volume is the same, the reflections from a sample of good crystalline quality are narrower and more intense than reflections from a sample of poor quality. In Fig. 2, the intensities and the full width at half maximum (FWHM in the  $\theta$ - $2\theta$  direction) of the MnPd(001) and MnPd(200) reflections versus the deposition temperature are shown. As seen in the figure, the intensity of the MnPd(200) reflection decreases while the FWHM increases with increasing temperature. The MnPd(001) reflection exhibits the opposite behavior: the intensity increases while the FWHM decreases. Two main conclusions can be drawn from the data. The first one is that the crystalline quality decreases when both crystallographic orientations are present, as indicated by the increased FWHM in the temperature range 200–350 °C. Preliminary TEM results show that both the MnPd and the Fe have uniform layer thicknesses. Thus, the change in peak width is therefore most likely due to a change in crystalline quality and not to a change in the thickness of the layers. The second conclusion is that between 350 and 450 °C, the orientation changes abruptly from a mixture of both *a* axis and *c* axis to a pure *c*-axis orientation. Chemical ordering requires interdiffusion, which is a strongly temperature-dependent process. Thus, a disordered *a*-axis oriented MnPd film is obtained at low temperatures where diffusion is limited. At high temperatures, on the other hand, during deposition the atoms can diffuse within and between different atomic layers, which facilitates the formation of a chemically ordered *c*-axis orientation. The magnitude of the exchange bias depends on the crystalline quality and the crystallographic orientation of the MnPd film in MnPd/Fe bilayers.<sup>6</sup> Bilayers with a chemically ordered *a*-axis orientation show exchange bias whereas disordered ones do not. Moreover, there is also a distinct difference in the magnitude of the exchange bias between the two orien-

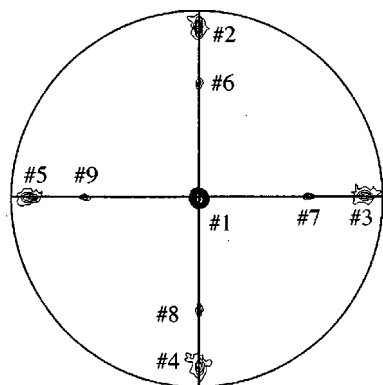


FIG. 3. A  $\text{MnPd}_{(002)}$  XRD texture scan from a  $\text{Au}(20 \text{ \AA})/\text{MnPd}(315 \text{ \AA})/\text{Fe}(73 \text{ \AA})$  bilayer deposited at  $400 \text{ }^\circ\text{C}$ . Reflection no. 1 originates from the  $c$ -axis orientation while nos. 2–5 originate from the  $a$ -axis orientation. The other reflections (nos. 6–9) indicate that there is also an intermediate unit cell orientation with neither the  $c$  axis nor the  $a$  axis parallel to the film normal.

tations; the spin-compensated  $c$ -axis orientation exhibits a larger exchange bias than the uncompensated  $a$  axis.

A  $\text{MnPd}_{(002)}$  XRD texture scan from a  $\text{Au}(20 \text{ \AA})/\text{MnPd}(315 \text{ \AA})/\text{Fe}(73 \text{ \AA})/\text{MgO}$  bilayer deposited at  $400 \text{ }^\circ\text{C}$  is shown in Fig. 3. For a single-crystalline purely  $c$ -axis oriented film, only one reflection is expected (reflection no. 1). However, the texture scan exhibits eight additional reflections with a fourfold symmetry. Reflections nos. 2–5 originate from the  $a$ -axis oriented component of the film, whereas reflections nos. 6–9 indicate that there is also a third intermediate unit cell orientation with neither the  $c$  axis nor the  $a$  axis parallel to the film normal. The very large difference in intensity between reflection no. 1 and the other reflections shows that the  $\text{MnPd}$  film is predominantly  $c$ -axis oriented. Moreover, the fourfold symmetry of the  $\text{MnPd}_{(002)}$  pole figure and the twofold symmetry of the  $\text{MnPd}_{(200)}$  (or  $\text{MnPd}_{(020)}$ ) atomic plane indicate a twinned crystal structure of the  $a$ -axis component as discussed above. A  $\text{MnPd}_{(202)}$  pole figure is shown in Fig. 4. Only four reflections (nos. 1–4) are expected for a single-crystalline  $c$ -axis oriented film. The additional reflections are very weak compared to

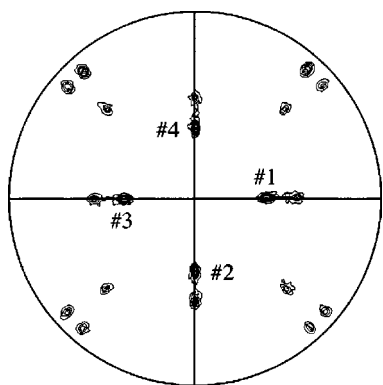


FIG. 4. A  $\text{MnPd}_{(202)}$  XRD texture scan from a  $\text{Au}(20 \text{ \AA})/\text{MnPd}(315 \text{ \AA})/\text{Fe}(73 \text{ \AA})$  bilayer deposited at  $400 \text{ }^\circ\text{C}$ . Reflections nos. 1–4 originate from the  $c$ -axis oriented component of the  $\text{MnPd}$  film. The other reflections in the pole figure indicate a complicated crystalline structure with the  $a$  and the  $c$  axis oriented in multiple directions.

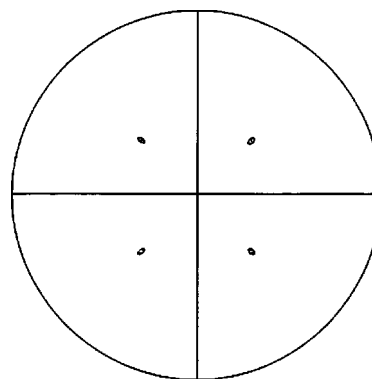


FIG. 5.  $\text{Fe}_{(202)}$  pole figure from a  $\text{Au}(20 \text{ \AA})/\text{MnPd}(315 \text{ \AA})/\text{Fe}(73 \text{ \AA})$  bilayer deposited at  $400 \text{ }^\circ\text{C}$ . Four reflections with a fourfold symmetry are seen indicating a single-crystalline  $\text{Fe}_{(001)}$  oriented film.

reflections nos. 1–4 but they indicate a complicated crystalline structure with the  $a$  and the  $c$  axis oriented in multiple directions.  $\text{MnPd}$  films deposited at  $500 \text{ }^\circ\text{C}$  do not exhibit these additional reflections; they are single-crystalline and purely  $c$ -axis oriented. The  $\text{Fe}_{(202)}$  pole figure seen in Fig. 5 exhibits four reflections with a fourfold symmetry as expected for a single-crystalline  $\text{Fe}_{(001)}$  film. As seen in the figure, the  $\text{Fe}$  unit cell is rotated by  $45^\circ$  with respect to the  $\text{MnPd}$  unit cell. It should be noted that an XRD measurement furnishes average structural information over a volume which is much larger than the unit cell. Hence, in order to determine the crystalline structure at length scales comparable to the atomic distance, a characterization method such as TEM must be used; such work is in progress.  $\text{MnPd}$  is an ordered antiferromagnet only if it is chemically ordered. It is not clear how a mixture of both  $a$ - and  $c$ -axis orientation affects the magnetic properties of the  $\text{MnPd}/\text{Fe}$  bilayers. However, the XRD measurements strongly suggest that  $\text{MnPd}$  preferentially grows as either an  $a$ - or  $c$ -axis oriented film on  $\text{Fe}_{(001)}$ ; when both orientations are present, one of them dominates. Thus, it is probable that the influence of the  $a$ -axis component in  $c$ -axis oriented films and vice versa is small.

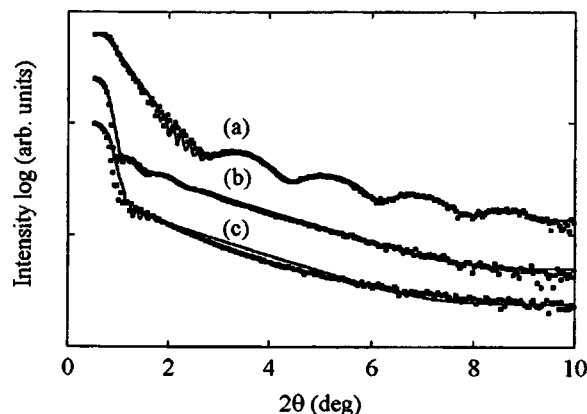


FIG. 6. Low-angle XRD data from three different samples: (a)  $\text{MnPd}/\text{Fe}$  bilayer deposited at  $400 \text{ }^\circ\text{C}$ , (b)  $\text{MnPd}/\text{Fe}$  bilayer deposited at  $500 \text{ }^\circ\text{C}$ , and (c) an  $\text{Fe}/\text{MnPd}$  bilayer deposited at  $400 \text{ }^\circ\text{C}$ . All three samples have the same nominal layer thicknesses.

Figure 6 shows XRD reflectivity scans from two MnPd/Fe (MnPd deposited on Fe) bilayers, deposited at 400 °C (a) and 500 °C (b) and one Fe/MnPd (Fe deposited on MnPd) bilayer (c) deposited at 400 °C. The data in Fig. 6(a) was fit to a Parratt model<sup>8</sup> with the following result: Au(30 Å)/MnPd(450 Å)/Fe(50 Å). All three samples have the same nominal layer thicknesses. Finite thickness oscillations with two different wavelengths are clearly distinguishable; the short-wavelength oscillations are due to the total thickness of the film, while the longer ones arise from the Fe layer. The fit also indicates a MnPd/Fe interface roughness of the order of 2.5 Å. It should be emphasized that this is an average value over a lateral length scale of the order of several hundred angstroms. A reflectivity scan measures both interface roughness and interdiffusion and it is therefore difficult to differentiate between these two types of interface disorder. Finite thickness oscillations are sensitive to interface disorder, thus the absence of these oscillations in Figs. 6(b) and 6(c) implies rough and diffuse interfaces in these two samples. The reflectivity data indicates that the interface roughness is as large as ~12 Å (b) and ~15 Å (c), respectively. Generally, interface roughness decreases with increasing deposition temperature until interdiffusion between the different layers is initiated.<sup>9</sup> The temperature at which this occurs depends on the materials used but also in which order they are deposited.<sup>10</sup> The reflectivity data suggest that interdiffusion is initiated at the MnPd/Fe interface between 400 and 500 °C. Furthermore, the very large interface roughness in the Fe/MnPd bilayer grown at 400 °C clearly shows that depositing Fe on MnPd is not the same as depositing MnPd on Fe; interdiffusion is initiated at the Fe/MnPd interface at a lower growth temperature as compared to the MnPd/Fe interface. The most probable explanation is a combination of a relatively high deposition temperature and a large difference in surface energy between the Fe<sub>(001)</sub> and the MnPd<sub>(001)</sub> surface. Interdiffusion at the MnPd/Fe interface is not energetically favorable during growth if the Fe<sub>(001)</sub> surface energy is larger than the MnPd<sub>(001)</sub>, while it is favorable at the Fe/MnPd interface.<sup>11</sup>

Exchange bias is an interface effect; the ferromagnetic and the antiferromagnetic layers are exchange coupled at the interface between the two materials. This makes the exchange bias effect sensitive to interface disorder such as roughness and interdiffusion. The two MnPd/Fe bilayers exhibit a very different magnetic behavior. Both samples show an exchange bias effect, -160 Oe (400 °C) and -90 Oe (500 °C). However, the bilayer deposited at 500 °C exhibits a significantly larger coercivity than the bilayer deposited at 400 °C (510 Oe compared to 110 Oe). For comparison, the coercivity for a pure single-crystalline Fe<sub>(001)</sub> film is of the order of 10–20 Oe. The differences are attributed to the large difference in interface disorder. It is not understood exactly how interface disorder affects the FM/AFM exchange coupling and why in some cases it decreases the exchange bias

and in others it increases.<sup>3,4</sup> A strong relationship between chemical order, crystal structure, interface disorder, and exchange bias has also been found in many other systems; two examples are MnPt/Co and MnPt/Py.<sup>12,13</sup> MnPt has the same crystal structure and almost the same lattice parameters as MnPd but a higher Néel temperature (700 °C), and the two magnetic easy directions are perpendicular to the (001) plane.<sup>5</sup>

## CONCLUSIONS

The orientation of the MnPd unit cell depends on the deposition temperature. Below 100 °C, a twinned *a*-axis oriented MnPd film is obtained while a single-crystalline *c*-axis film is obtained above 450 °C. Intermediate temperatures yield a mixture of both orientations with a poor crystalline quality.

The quality of the interface between MnPd and Fe depends strongly on the deposition temperature and in which order the two materials are deposited. Interdiffusion is initiated at the MnPd/Fe interface between 400 and 500 °C. The results show that the Fe/MnPd interface is more sensitive to interdiffusion than the MnPd/Fe interface.

The magnitude of the exchange bias and the coercivity is very sensitive to the FM/AFM interface structure. The exchange bias decreases while the coercivity increases with increasing interface disorder.

## ACKNOWLEDGMENTS

This work was supported by the DOE Materials Science Division under Grant No. DE-FG03-02ER45987 and by the Campbell Endowment at UW. The research described in this paper was performed in part at the Environmental Molecular Sciences Laboratory, a national scientific user facility sponsored by the U.S. Department of Energy's Office of Biological and Environmental Research and located at Pacific Northwest National Laboratory in Richland, WA.

<sup>1</sup>W. H. Meiklejohn and C. P. Bean, Phys. Rev. **102**, 1413 (1956).

<sup>2</sup>W. H. Meiklejohn and C. P. Bean, Phys. Rev. **105**, 904 (1957).

<sup>3</sup>J. Nogués and I. K. Schuller, J. Magn. Magn. Mater. **192**, 203 (1999).

<sup>4</sup>A. E. Berkowitz and K. Takano, J. Magn. Magn. Mater. **200**, 552 (1999).

<sup>5</sup>H. P. J. Wijn, *Magnetic Properties of Metals* (Springer, New York, 1991).

<sup>6</sup>N. Cheng, J. P. Ahn, and Kannan M. Krishnan, J. Appl. Phys. **89**, 6597 (2001).

<sup>7</sup>R. F. C. Farrow, R. F. Marks, M. F. Toney, S. David, A. J. Kellock, J. A. Borchers, K. V. O'Donovan, and D. J. Smith, Appl. Phys. Lett. **80**, 808 (2002).

<sup>8</sup>L. G. Parratt, Phys. Rev. **95**, 359 (1954).

<sup>9</sup>P. Isberg, E. B. Svedberg, B. Hjörvarsson, R. Wäppling, and L. Hultman, Vacuum **48**, 483 (1997).

<sup>10</sup>P. Blomqvist and R. Wäppling, J. Cryst. Growth **252**, 120 (2003).

<sup>11</sup>D. Lederman, J. Nogués, and I. K. Schuller, Phys. Rev. B **56**, 2332 (1997).

<sup>12</sup>Erie H. Morales, Y. Wang, D. Lederman, A. J. Kellock, and M. J. Carey, J. Appl. Phys. **93**, 4729 (2003).

<sup>13</sup>Kannan M. Krishnan, C. Nelson, C. J. Echer, R. F. C. Farrow, R. F. Marks, and A. J. Kellock, J. Appl. Phys. **83**, 6810 (1998).